Journal of Physiology and Biochemistry (2019) 75:39–51
https://doi.org/10.1007/s13105-018-0648-7

ORIGINAL ARTICLE

Effects of resveratrol on regulation on UCP2 and cardiac function in diabetic rats

Jiayu Diao[1] · Jin Wei[2] · Rui Yan[3] · Gang Fan[2] · Lin Lin[2] · Mengjie Chen[2]

Received: 16 March 2018 / Accepted: 5 September 2018 / Published online: 17 September 2018
© University of Navarra 2018

Abstract

Mitochondrial dysfunction is essential in the development and prognosis of diabetic cardiomyopathy (DCM). Resveratrol (RES) is thought as a mitochondrial protector. In this study, we hypothesized that RES may ameliorate mitochondrial function and consequently improve cardiac function in diabetic rats, and uncoupling protein 2 (UCP2) was involved in the protective effects of RES on DCM. Thirty rats were divided into three groups: normal control, DCM, and DCM+RES groups. DCM was induced by high-fat diet and streptozotocin (STZ) intraperitoneal injection, the rats in DCM+RES group received RES gavage for 16 weeks. RES improved the insulin resistance, and reduced the level of triglyceride, cholesterol, and low density lipoprotein cholesterol (LDLc) in DCM rats (all $P < 0.05$). Echocardiographic and hemodynamic studies revealed that RES treatment reversed the impaired diastolic and systolic cardiac function in DCM rats. Meanwhile, RES improved myocardial structural disorder and fibrosis, reserved mitochondrial membrane potential level ($P < 0.05$), and suppressed myocardial apoptosis in DCM rats ($P < 0.05$). Myocardial mitochondrial respiratory enzyme activities were improved by RES treatment in DCM rats ($P < 0.05$), accompanied with attenuated reactive oxygen species (ROS) generation ($P < 0.05$). The expression of UCP2 was further increased by RES treatment both in the myocardium of DCM rats ($P < 0.05$) and in the H9c2 cardiomyocytes incubated with high-glucose ($P < 0.05$). The protective effects of RES on high glucose-induced ROS generation, MPTP opening, Cyto c release, and cell apoptosis were all blunted by inhibiting the expression of UCP2 (all $P < 0.05$). In conclusion, RES treatment improved cardiac function and inhibited cardiomyocyte apoptosis, involving in ameliorating mitochondrial function in diabetic rats. UCP2 mediated the protective effects of RES on diabetic hearts.

Keywords Resveratrol · Diabetic cardiomyopathy · Mitochondria · Uncoupling protein 2

Abbreviations

COX	Cytochrome c oxidase
EF	Ejection fraction
FS	Fractional shortening
GLUT4	Glucose transporter 4
HG	High-glucose
LDLc	Low density lipoprotein cholesterol
LVEDd	Left ventricular end-diastolic dimension
LVEDv	Left ventricular end-diastolic volume
LVESd	Left ventricular end-systolic dimension
LVESv	Left ventricular end-systolic volume
LVEDP	Left ventricular end-diastolic pressure
LVSP	Left ventricular systolic pressure
MMP	Mitochondrial membrane potential
MPTP	Mitochondrial permeability transition pore
NC	Normal control
ROS	Reactive oxygen species
SDH	Succinate dehydrogenase
Sir2	Silent information regulatory 2
STZ	Streptozotocin
UCP2	Uncoupling protein 2

✉ Jiayu Diao
diaojiayu2014@stu.xjtu.edu.cn

[1] Department of Cardiovascular Medicine, Shaanxi Provincial People's Hospital, Xi'an 710000, China

[2] Department of Cardiovascular Medicine, The Second Affiliated Hospital, Xi'an Jiaotong University, Xi'an 710000, China

[3] Department of Cardiovascular Medicine, Beijing Luhe Hospital, Capital Medical University, Beijing 101100, China

Introduction

Diabetic cardiomyopathy (DCM) is a complex complication in diabetes patients with adverse prognosis [9, 27]. DCM is characterized by left ventricular hypertrophy and interstitial fibrosis, with early diastolic dysfunction, accompanied with or without systolic dysfunction [14, 18]. However, the pathological mechanism of DCM has not been completely understood, and the effects of current therapeutic approaches on DCM are unsatisfied [15].

Mitochondria play an essential role in maintaining normal heart function, as the center of energy metabolism and the major source of reactive oxygen species (ROS) generation [24]. In diabetic hearts, mitochondrial abnormalities, including altered energy metabolism, oxidative stress, mitochondrial calcium imbalance, and increased apoptosis were proved in previous studies [1, 12, 21]. Emerging evidences suggested that mitochondrial dysfunction seemed as a key contributor to the diabetes-induced cardiac damage [22, 38]. The approaches targeting mitochondria are promising for the treatment and prevention of DCM.

In recent years, medicinal plants with hypoglycemic properties for the management of diabetic complications have become increasingly attractive. Resveratrol (RES) is a group of polyphenolic compounds found mainly in plants, including grapes, blue berries, giant knotweed, and polygonum nigrumis, and is known as its antioxidant, anti-inflammation, and anti-tumor activities [3, 4, 16]. RES can promote mitochondrial biosynthesis and inhibit mitochondrial excessive division, and is considered as a protective agent for mitochondria [7]. Accordingly, RES may have a therapeutic potential for DCM by ameliorating mitochondrial function.

Uncoupling protein 2 (UCP2) is a proton transporter, which is located in the mitochondrial inner membrane. UCP2 can cause H^+ leakage from mitochondrial membrane spaces into the matrix, and reduce the generation of ROS, thereby regulate mitochondrial function [5, 19]. These features of UCP2 strongly suggested that UCP2 may improve mitochondrial function by suppressing ROS production in diabetic hearts. And the expression of UCP2 can be up-regulated by RES in diabetic liver and skeletal muscle [10]. But there is no data about whether UCP2 is involved in the effects of RES.

Therefore, in the present study, we hypothesized that RES may regulate UCP2, and have protective effects on mitochondrial and cardiac function in diabetic rats.

Methods

Animals

All animal experimental procedures were approved by the Institutional Animal Research and Ethics Committee of Xi'an Jiaotong University (SCXK2007-001). Thirty male Sprague-Dawley rats (100–150 g) obtained from the Animal Center of Xi'an Jiaotong University were used in the experiments. All applicable international and national guidelines for the care and use of animals were followed.

Diabetes induction

Diabetic rats were induced by high-fat diet and streptozotocin (STZ, Sigma-Aldrich, St. Louis, MO, USA) intraperitoneal injection. After adaptive feeding for 1 week, diabetic rats received high-fat diet with 40% fat, 13% protein, 40% carbohydrate, and 7% others. After high-fat feeding for 4 weeks, STZ were intraperitoneally injected at a dose of 30 mg/kg body weight. Age-matched control rats received only standard diet (10% fat, 22% protein, 60% carbohydrate, and 8% others) and sodium-citrate buffer injection. Blood glucose levels were measured in tail vein blood 1 week after STZ or sodium-citrate buffer injection. The rats with high-fat diet and STZ injection were considered as diabetic with fasting blood glucose over 200 mg/dl.

Experimental protocol

Thirty rats were randomly divided into three groups according to treatments as follows (ten rats per group): (1) control; (2) DCM; and (3) DCM+RES. Four weeks after STZ injection, the rats in DCM+RES group received 10 mg/kg/d of RES. RES was dissolved with dimethyl sulfoxide and administered via gavage once a day for eight consecutive weeks, at a volume less than 0.1 mL/100 g rat weight. While the rats in the control and DCM groups received saline gavage.

Blood glucose, plasma insulin, and lipid measurements

Rats were fasted for 8 h, and tail vein blood samples were collected. Blood glucose levels were measured with animal micro blood glucose detector (Alpha-TRAK, Abbott Laboratories, USA). Plasma insulin and triglyceride, cholesterol, and low density lipoprotein cholesterol (LDLc) contents were determined by using ELISA kits (Alpco Diagnostic, USA). The insulin resistance index was calculated as (fasting glucose × fasting insulin) / 22.5.

Echocardiographic study

Echocardiographic study was performed by an investigator blinded to the animal treatments. The two-dimensional echocardiographic system, equipped with a 12- to 4-MHz transducer (Philips iE33, Netherlands), was used to evaluated the cardiac structure and function. The cardiac parameters

including left ventricular systolic and diastolic index were measured and calculated.

Hemodynamic studies

After anesthetizing with intraperitoneal injection of chloral hydrate, a PE-50 catheter, which connected with a pressure-electricity transducer, was inserted into the left ventricle (LV) through the right carotid artery of rats. LV systolic and diastolic pressures, as well as the maximum and minimum rates of LV pressure development (dP/dt), were measured and recorded with the Power Lab 4.12 system (AD instrument, Sydney, Australia) using Chart 5.0 software.

Cardiac hematoxylin-eosin (HE) and Masson's staining

The LV myocardium was fixed in 10% neural buffered formalin for histology analysis. Sectioning of paraffin-embedded myocardial blocks at 3 μm was performed. To detect the remodeling and fibrosis in the LV myocardium, the paraffin sections were stained with HE and Masson's trichrome, respectively, and were observed using optical microscopy (Olympus, Bx 43, Tokyo, Japan).

TUNEL staining

Myocardial apoptosis in situ was detected by terminal deoxynucleotidyl transferase (TdT)-mediated dUTP nick end labeling (TUNEL, Promega Bitotech Co., Ltd., Madison, USA). Briefly, the paraffin sections were incubated with proteinase K at room temperature for 10 min, and subsequently permeabilized in 0.25% Triton X-100 for 10 min and incubated with TUNEL reaction mixture for 90 min and 4′,6-diamidino-2-phenylindole (DAPI, Boster, Wuhan, China) for 5 min at 37 °C in the dark. All the steps above were separated by sufficiently washing with phosphate buffer saline (PBS). Finally, six sections from each groups, and three high power fields from each section were randomly chosen and photographed. TUNEL-positive cells were calculated for every section by fluorescence microscope (Olympus, Bx 50-FLA, Japan).

Western-blot

Myocardium and cell samples were lysed with RIPA lysis buffer (Beyotime Biotechnology Co., Hangzhou, China). The homogenates of the lysates were centrifuged at 16,000*g* for 20 min at 4 °C. Supernatants for protein concentration assessment were collected. Equal amounts of protein were electrophoresed on sodium dodecyl sulfate-polycrylamide gel electrophoresis and then transferred onto an equilibrated polyvinylidene fluoride (PVDF) membrane. The PVDF membrane was incubated with 5% skimmed milk in PBS-Tween-20 for 2 h and then with the primary antibodies against UCP2 (1:1000), Bcl-2 (1:1000), cytochrome c (1:1000), β-actin (1:2000), and COX IV (1:2000) overnight at 4 °C. The membrane was washed with PBST three times and incubated with the secondary antibodies (peroxidase-conjugated goat anti-rabbit IgG) at a dilution of 1:2000 for 2 h. Subsequently, blots were visualized with the enhanced chemiluminescence detection system. Finally, the digital images were analyzed using Image-Pro Plus software 6.0 (Olympus, 12119-987). In these experiments, β-actin and COX IV were used as internal control. The antibody against UCP2 was purchased from Cell Signaling Technology (Danvers, USA). The antibodies against Bcl-2, Cyto c, β-actin, and COX IV were purchased from Proteintech (Rosemont, USA).

Respiratory enzyme activity measurement in myocardium

Succinate dehydrogenase (SDH) and cytochrome c oxidase (COX) activities were measured using a SDH assay kit (Jiancheng Bioengineering Ins., Nanjing, China) and COX assay kit (Jiancheng) following the manufacturer's instructions. For SDH activity measurement, the homogenized myocardium was centrifuged at 1600*g* for 10 min. The supernatant was mixed with 37 °C SDH working liquid for 5 min, then SDH activity was quantitatively determined due to the changes of absorbance from 5 s to 65 s under the spectrophotometer (TianPu 722, Shanghai, China) at 600 nm. For COX activity measurement, the supernatant was mixed with COX working liquid at room temperature for 3 min, COX activity was quantitatively determined due to the changes of absorbance from 0 s to 60s under the spectrophotometer (TianPu 722) at 550 nm.

Cardiac mitochondria isolation

Mitochondria were isolated by using tissue mitochondria isolation kit (Beyotime). According to the manufacturer's instructions, the myocardium was incubated with PBS on the ice for 3 min, then centrifuged at 600*g* for 10 s. The precipitation was collected and digested with pancreatic enzyme for 10 min on ice, then centrifuged at 600*g* for 10 s. Collect the precipitation and centrifuge it with mitochondria-separating agent at 600*g* for 10 s. Then, the precipitation was homogenized with separating agent on ice. Next, the homogenate was centrifuged at 4 °C at 600*g* for 5 min. Finally, mitochondria fraction was obtained by centrifugation of supernatant at 11,000*g* for 10 min at 4 °C. The precipitation, mitochondria fraction, was stored with storage fluid at − 80 °C.

Mitochondrial membrane potential (MMP) measurement

MMP level was detected by using the lipophilic cationic probe, 5,6,6-tetrachloro-1,1,3,3-tetraethylbenzimidazolylcarbocyanine iodide (JC-1) (Beyotime). Once after the isolated fresh mitochondria mixed with JC-1 staining, a fluorescence microplate reader (Tecan Infinite M200, Switzerland) was used to assess the level of MMP according to the intensity of green and red JC-1 fluorescence.

ROS measurement in myocardium

ROS generation in myocardium was measured with dihydroethidium (DHE) labeling (Sigma-Aldrich). According to the manufacturer's instructions, DHE staining was dissolved in Krebs solution with the concentration of 0.04 M. Then, the surface of frozen sections with DHE staining was covered. After that, the samples were incubated for 30 min at 37 °C in the dark. Finally, wash the samples with fresh Krebs for three times. The red fluorescence was observed immediately under a fluorescence microscope (Olympus) with excitation wavelength of 510 nm and emission wavelength of 610 nm. Six sections from each groups, and three high power fields from each section were randomly chosen and photographed. Image-Pro Plus6.0 image analysis software was used to analyze the fluorescence results, and the intensity of red fluorescence represented the level of ROS in myocardium.

Cell culture and treatments

The H9c2 cardiomyocytes were obtained from the Cell Bank of Shanghai Institute of Bio-chemistry and Cell Biology, Chinese Academy of Sciences (Shanghai, China), cultured in 90% DMEM (Hyclone, Logan, USA) with 10% FBS at 37 °C. When they reached confluence, the cells were divided to four groups based on experimental need: normal control group (NC), cells were incubated with glucose 5.5 mM; high-glucose group (HG), cells were incubated with glucose 33 mM for 48 h; HG+RES group, cells were pretreated with 25 μM RES for 6 h, and then incubated with HG for additional 48 h; and HG+RES+UCP2siRNA group, cells were transfected with UCP2siRNA, and pretreated with 25 μM RES for 6 h, then incubated with HG for additional 48 h.

siRNA transient transfection

UCP2siRNA was synthesized from GenePharma (Shanghai, China). The sequences of UCP2siRNA were as follows: 5′-GCCUGUAUGAUUCUGUCAAACTT-3′ (forward) and 5′-GUUUGACAGAAUCAUACAGGCTT-3′ (reverse). The UCP2siRNA was introduced into H9c2 cells using Lipofectamine 2000. The cells were seeded in 12-well plates 24 h before transfection. Then, the cells were transfected with the mixture of 100 μL siRNA and 100 μL Lipofectamine 2000. Forty-eight hours after transfection, the cells were harvested.

Mitochondrial permeability transition pore (MPTP) measurement in H9c2 cells

The opening of MPTP was detected by Calcein-AM labeling (Genmed Scientifics, USA). First, add 37 °C preheated cleaning liquid to wash cells in 12-well plates. Then, add 500 μL staining solution to each well, shake the culture plate gently. The cells were incubated under 37 °C for 20 min in the dark. Finally, wash the cell in plates with 37 °C preheated cleaning liquid for three times. The green fluorescence was observed immediately under a fluorescence microscope (Olympus). Six sections from each groups, and three fields from each section were randomly chosen and photographed. Image-Pro Plus6.0 image analysis software was used to analyze the fluorescence results; the decreased intensity of green fluorescence indicates that the opening of MPTP is enhanced.

ROS measurement in H9c2 cells

The ROS generation in H9c2 cells was detected by DHFH-DA labeling (Beyotime). First, wash cells in 12-well plates with PBS. Then, add 500 μL DCFH-DA staining solution to each well. The cells were incubated under 37 °C for 30 min in the dark. Finally, wash the cells with serum-free medium for three times. The green fluorescence was observed immediately under a fluorescence microscope (Olympus). Six sections from each group and three fields from each section were randomly chosen and photographed. Image-Pro Plus6.0 image analysis software was used to analyze the intensity of green fluorescence which indicates the level of ROS generation.

Apoptosis measurement in H9c2 cells

Apoptosis cells were identified by Annexin V-FITC Apoptosis Detection Kits (Beyotime). 1×10^6 cells were harvested from 6-well plate, and washed at 4 °C PBS twice. Cells were suspended in 500 μL Bingding Buffer (1×), then added 5 μL Annexin V-FITC and 10 μL PI, and incubated at room temperature for 15 min in the dark. FACSCalibur flow cytometry (Becton, Dickinson and Company, USA) was used to analyze the level of cardiomyocyte apoptosis by containing Annexin V^+ cell population.

Statistical analysis

Data were expressed as means ± standard deviation, and statistical analysis was performed using SPSS 18.0. Data are represented by mean ± standard deviation. Comparisons between groups were evaluated using a single factor analysis of variance (one-way, ANOVA), the differences between two groups was used of LSD-t test. A value of $P < 0.05$ was considered as statistically significant.

Results

The effect of RES on blood glucose, plasma insulin, and lipids in diabetic rats

After 16 weeks of treatment with high-fat diet and STZ intraperitoneal injection, a DCM model was successfully induced. At the end of the experimental period, the body weight in DCM group was lower compared to that in control group ($P < 0.05$, Fig. 1a), but there was no difference of body weight between DCM and DCM+RES groups ($P > 0.05$, Fig. 1a). Fasting blood glucose and insulin levels in DCM group were both much higher than those in control group, respectively (both $P < 0.05$, Fig. 1b, c). RES treatment lowered the glucose and insulin levels in DCM rats (both $P < 0.05$, Fig.1b, c). Thus, RES improved the insulin resistance in DCM rats, which was indicated by insulin resistance index ($P < 0.05$, Fig. 1d). Plasma triglyceride, cholesterol, and LDLc contents were all significantly higher in DCM group compared to those in control group (all $P < 0.05$, Fig. 1e–g). Meanwhile, RES lowered the triglyceride, cholesterol, and LDLc levels in DCM rats (all $P < 0.05$, Fig. 1e–g).

The effect of RES on cardiac function and histopathology in diabetic rats

As shown in Table 1, the echocardiographic study revealed significant dilation of left ventricle chambers in the DCM group, which was characterized by significantly increased left ventricular end-diastolic dimension (LVEDd), left ventricular end-diastolic volume (LVEDv), left ventricular end-systolic dimension (LVESd), and left ventricular end-systolic volume (LVESv) compared with control group. In addition, ejection fraction% (EF%) and fractional shortening% (FS%) were significantly reduced in DCM group. The hemodynamic studies showed marked decrease of left ventricular systolic pressure (LVSP) and first derivative of pressure (dp/dt), but significant increase of left ventricular end-diastolic pressure (LVEDP) in DCM group, which indicated that the systolic function of the heart was impaired. In comparison with the DCM group, LVEDd, LVEDv, LVESd, and LVESv were all lower in the DCM+RES group; EF%, FS%, LVSP, and dp/dt were significantly higher in the DCM+RES group. Consequently, RES treatment could ameliorate the impaired cardiac systolic and diastolic functions in DCM rats.

Under optical microscopic observation, the significant degeneration and disorganization of myocardial fibers, cardiomyocytes vacuole degeneration, and myocardial interstitial edema were obvious in the DCM rats. While in the control and DCM+RES groups, the myocardial fibers were arranged regularly, and little cardiomyocyte vacuole and interstitial edema have been observed (Fig. 2a). Myocardial collagen tissue was obviously increased and disarranged in the DCM group, but were sparse with regular array in the control and DCM+RES groups (Fig. 2A). Further quantitative analysis showed that collagen volume fraction in the DCM group

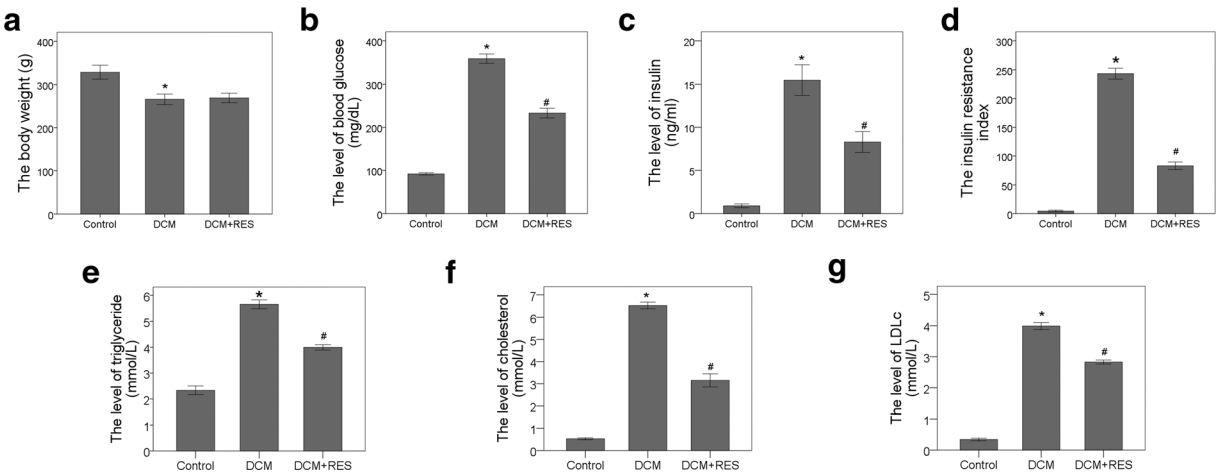

Fig. 1 RES improved insulin resistance and lowered the plasma lipid levels in DCM rats. **a** RES treatment had no effect on the body weight in DCM rats. RES reduced blood glucose (**b**) and insulin (**c**) levels, and improved insulin resistance (**d**) in DCM rats. RES lowered the levels of plasma triglyceride (**e**), cholesterol (**f**), and LDLc (**g**) in DCM rats. LDLc, low density lipoprotein cholesterol. * $P < 0.05$ versus the control group; # $P < 0.05$ versus the DCM group

Table 1 RES ameliorated impaired systolic and diastolic cardiac function in DCM rats

Parameter	Control ($n = 10$)	DCM ($n = 10$)	DCM+RES ($n = 10$)
Echocardiographic analysis			
LVEDd (mm)	6.58 ± 0.34	7.64 ± 0.62*	7.03 ± 0.21#
LVESd (mm)	4.83 ± 0.14	5.61 ± 0.11*	5.08 ± 0.09#
LVEDv	270 ± 11.6	328.6 ± 20.4*	284.5 ± 16.1#
LVESv	86.1 ± 7.9	121.3 ± 11.5*	104.7 ± 9.4#
EF (%)	76.5 ± 1.48	61.2 ± 2.45*	68.6 ± 1.82#
FS (%)	41.2 ± 1.61	34.6 ± 1.19*	38.1 ± 0.96#
Hemodynamic analysis			
dp/dtmax (mmHg/s)	8653 ± 433	5362 ± 341*	6969 ± 353#
dp/dtmin (mmHg/s)	7684 ± 561	5016 ± 382*	6541 ± 546#
LVSP (mmHg/s)	140 ± 7.68	113 ± 11.26*	129 ± 13.6#
LVEDP (mmHg/s)	− 1.42 ± 0.35	2.31 ± 0.84*	− 0.68 ± 0.57#

LVEDd left ventricular end-diastolic dimension, *LVEDv* left ventricular end-diastolic volume, *LVESd* left ventricular end-systolic dimension, *LVESv* left ventricular end-systolic volume, *EF* ejection fraction, *FS* fractional shortening, *dp/dt* first derivative of pressure, *LVSP* left ventricular systolic pressure, *LVEDP* left ventricular end-diastolic pressure

Data are represented by mean ± standard deviation. * $P < 0.05$ versus the control group; # $P < 0.05$ versus the DCM group

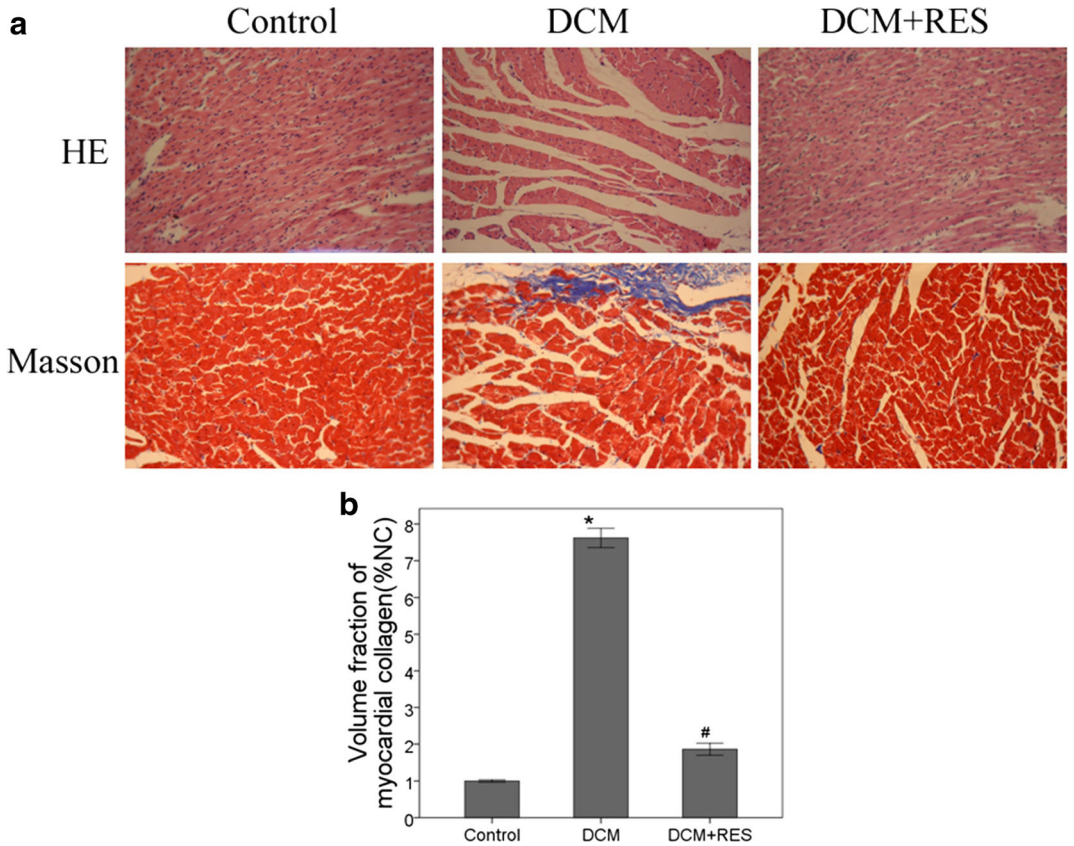

Fig. 2 RES improved left ventricular remolding and fibrosis in DCM rats. **a** Representative photomicrographs showed myocardial sections stained with HE (upper) and Masson's trichrome (bottom). **b** Quantitative analysis of collagen volume fraction in the control group, DCM group, and DCM+RES group. * $P < 0.05$ versus the control group; # $P < 0.05$ versus the DCM group

was significantly greater than that in the control and DCM+RES groups ($P < 0.05$, Fig. 2b).

The effect of RES on cardiomyocyte apoptosis in DCM rats

Reduction of MMP was thought as a sign of cell early apoptosis. The level of MMP in DCM group was notably decreased compared with the control group; While, RES treatment suppressed the decrease of MMP level in DCM rat hearts ($P < 0.05$, Fig. 3a).

Then, we assessed the myocardial apoptotic rate by TUNEL labeling. The myocardial apoptotic rate was higher in DCM group than that in control group, and it was lower in DCM+RES group than that in DCM group ($P < 0.05$, Fig. 3b).

Bcl-2 is one of the ultimate pathways of apoptosis, as an anti-apoptosis factor. The expression of Bcl-2 in DCM group was significantly decreased compared with the control group; while RES increased the Bcl-2 expression in DCM rat hearts ($P < 0.05$, Fig. 3c).

All the results indicated that RES treatment suppressed cardiomyocyte apoptosis in DCM.

The effect of RES on mitochondrial respiratory function and the generation of ROS in DCM rat hearts

We evaluated the mitochondrial function by assessing the activities of respiratory enzymes and the generation of ROS.

As shown in Fig. 4a, the activities of respiratory enzymes, SDH, and COX were both significantly decreased in DCM group compared with that in control group (both $P < 0.05$). RES treatment improved the activities of both SDH and COX in DCM rat hearts (both $P < 0.05$).

We detected the generation of ROS in myocardium by DHE labeling. The level of ROS was much higher in DCM group than in control group. In DCM+RES group, the generation of ROS was attenuated compared with DCM group ($P < 0.05$, Fig. 4b).

Together, RES ameliorated the mitochondrial respiratory function in DCM rat hearts, and reduced the generation of ROS.

The effect of RES on expression of UCP2 in cardiomyocytes

UCP2 plays an important role in regulating mitochondrial functions, based on suppressing ROS generation. In the rat hearts as shown in Fig. 5a, the expression of UCP2 was increased in DCM group compared with that in control group, RES treatment improved the expression of UCP2 in DCM rats further ($P < 0.05$).

In H9c2 cardiomyocytes, high-glucose incubation increased the expression of UCP2 compared with the NC group, and RES improved the expression of UCP2 further with a dose-dependent manner ($P < 0.05$, Fig. 5b).

UCP2 mediated the effects of RES on mitochondrial function in H9c2 cells

RES improved the cardiac function and up-regulated the expression of UCP2 in DCM rats. But whether UCP2 mediated the protective effects of RES on DCM is unknown. And what is the role?

UCP2siRNA was used to inhibit the expression of UCP2 in cells with RES treatment. As shown in Fig. 6a, b, RES treatment reserved the activities of respiratory enzymes, and suppressed the generation of ROS in H9c2 cells incubated with

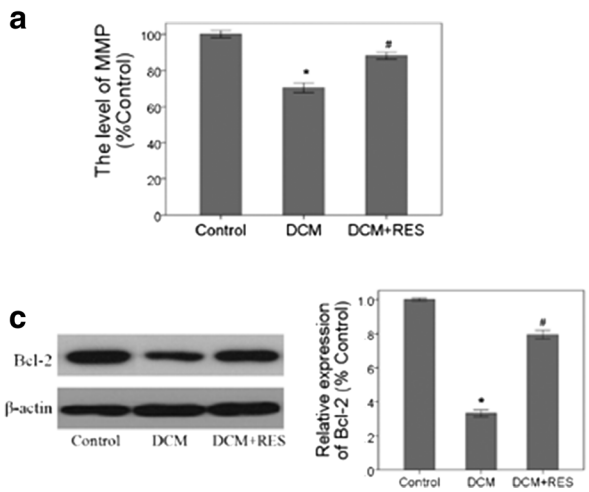

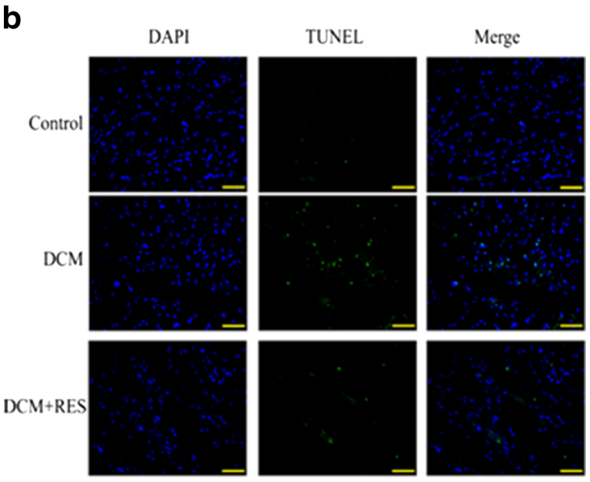

Fig. 3 RES suppressed cardiomyocyte apoptosis in DCM rats. **a** RES reserved the MMP level in DCM rat hearts. **b** RES reduced cardiomyocyte apoptotic rate in DCM rats. **c** RES increased Bcl-2 expression in DCM rat hearts. MMP, mitochondrial membrane potential. * $P < 0.05$ versus the control group; # $P < 0.05$ versus the DCM group

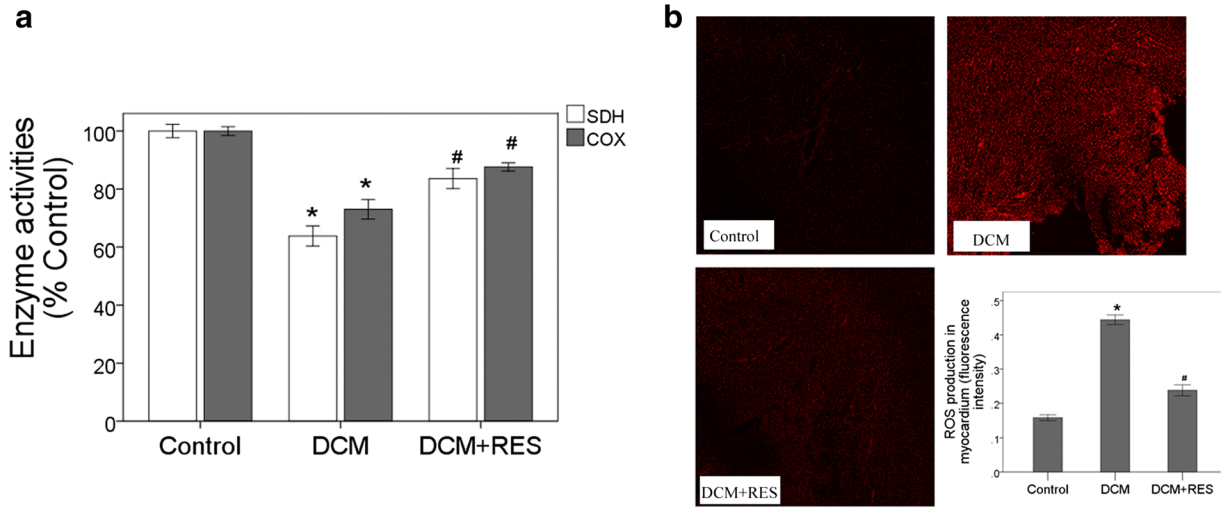

Fig. 4 RES ameliorated the mitochondrial respiratory enzyme activities (**a**) and reduced the generation of ROS (**b**) in DCM rat hearts. SDH, succinate dehydrogenase; COX, cytochrome c oxidase; ROS: reactive oxygen species. * $P < 0.05$ versus the control group; # $P < 0.05$ versus the DCM group

HG. But the effects of RES were blunted by inhibiting the expression of UCP2 in HG+RES+UCP2siRNA group ($P < 0.05$).

MPTP can be activated by ROS and sustained opening, which facilitates apoptotic factor release from the mitochondria. RES reduced the level of MPTP opening in H9c2 cells incubated with HG. But the effect of RES on inhibiting MPTP opening was reduced in HG+RES+UCP2siRNA group ($P < 0.05$, Fig. 6c).

Cyto c release from mitochondria resulted from MPTP opening is a sign of mitochondrial pathway apoptosis. Western-blot results revealed that Cyto c expression in mitochondria is lower in HG group than that in NC group. RES treatment restored the Ctyo c in mitochondria of cells incubated with HG, but the effect of RES was blunted by inhibiting the expression of UCP2 in HG+RES+UCP2siRNA group ($P < 0.05$, Fig. 6d).

Together, RES reduced the generation of ROS, lowered the level of MPTP opening, and subsequently inhibited Cyto c release from mitochondria in cardiomyocytes under high-glucose condition. And the effects of RES on ameliorating mitochondrial function are mediated by UCP2.

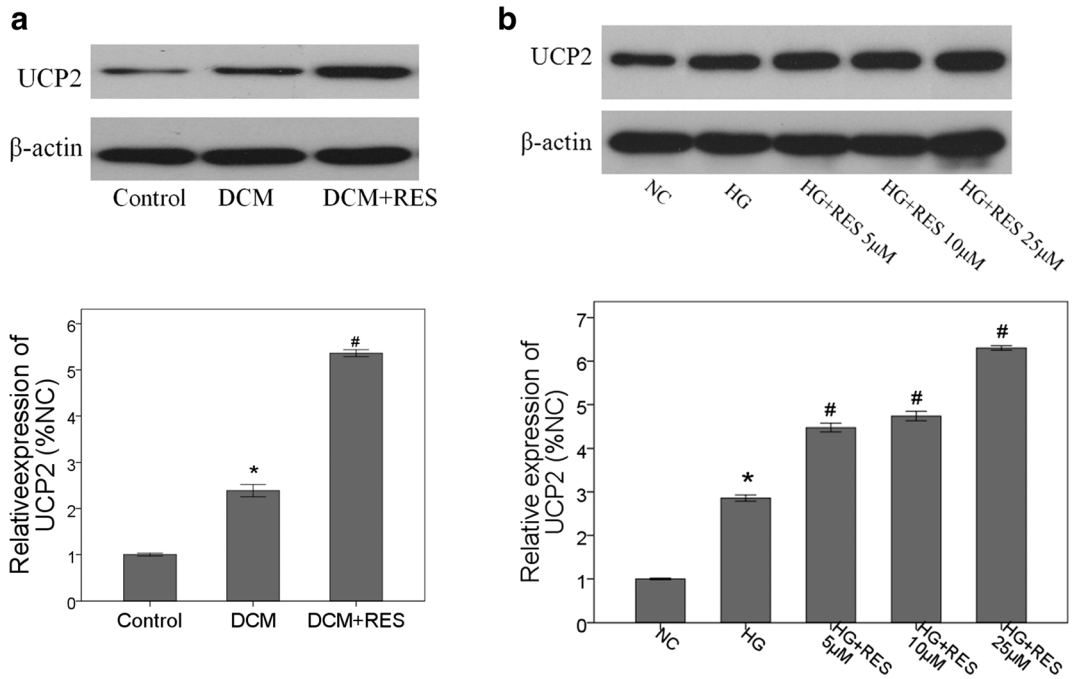

Fig. 5 RES improved the expression of UCP2 in the DCM rat hearts (**a**) and H9c2 cells incubated with high-glucose (**b**). NC: normal control; HG: high glucose; * $P < 0.05$ versus the control group; # $P < 0.05$ versus the DCM group

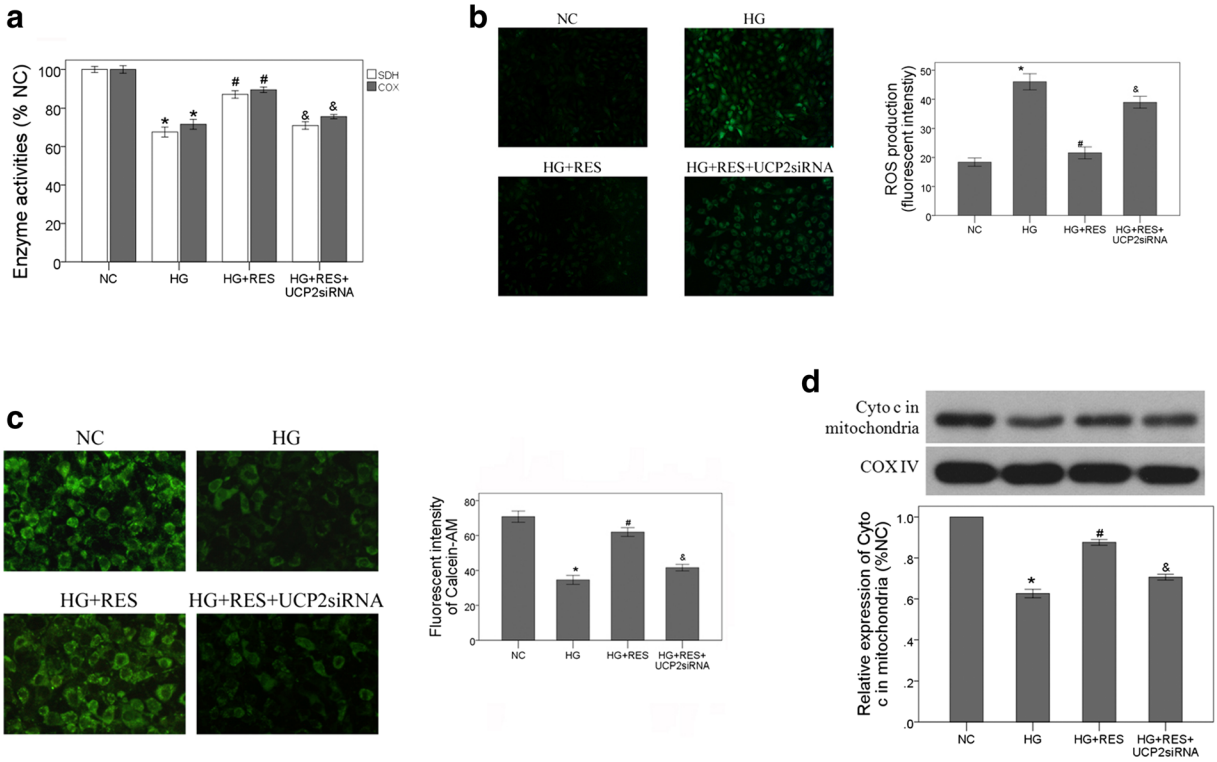

Fig. 6 RES ameliorated mitochondrial function mediated by UCP2 in cardiomyocytes. UCP2 mediated the effect of RES on reserving the activities of respiratory enzymes (**a**), reducing the generation of ROS (**b**), inhibiting the enhanced opening of MPTP (**c**), and the release of Cyto c from mitochondria (**d**) in cardiomyocytes. NC, normal control; HG, high glucose; SDH, succinate dehydrogenase; COX, cytochrome c oxidase; ROS: reactive oxygen species; MPTP, mitochondrial permeability transition pore; Cyto c, cytochrome c. * $P < 0.05$ versus the NC group; # $P < 0.05$ versus the HG group; & $P < 0.05$ versus the HG+RES group

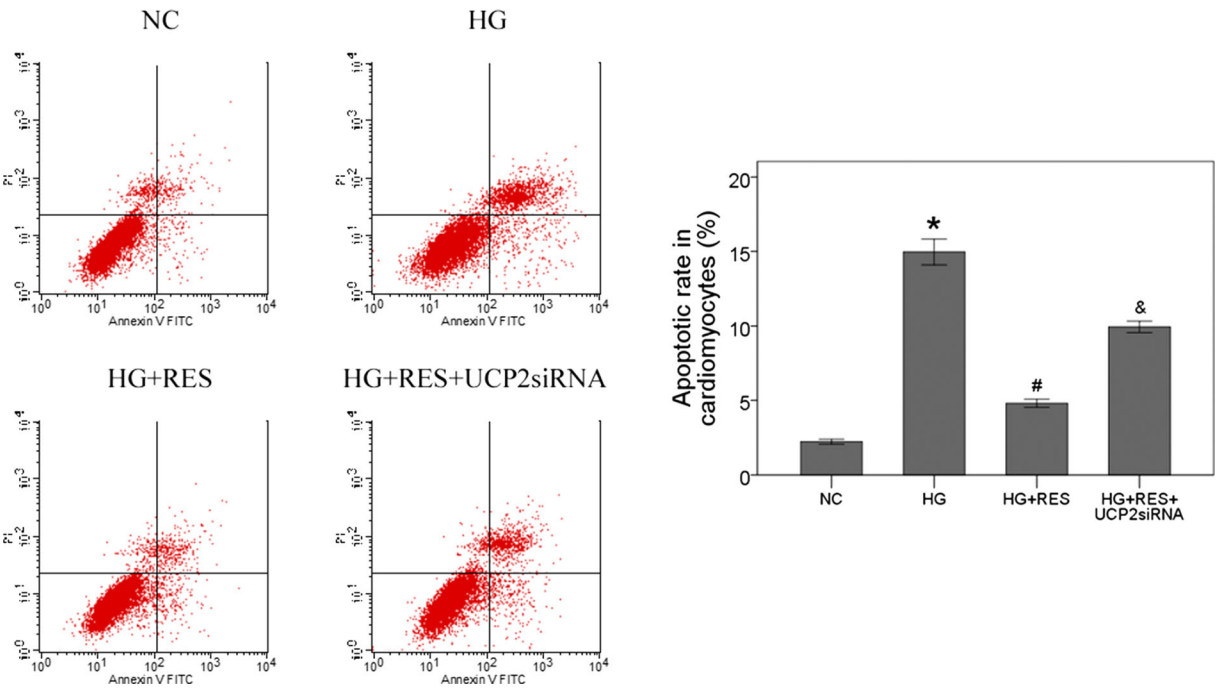

Fig. 7 RES suppressed HG-induced apoptosis mediated by UCP2 in cardiomyocytes. NC, normal control; HG, high glucose. * $P < 0.05$ versus the NC group; # $P < 0.05$ versus the HG group; and $P < 0.05$ versus the HG+RES group

UCP2 mediated the effect of RES on cardiomyocyte apoptosis

Finally, we assessed the apoptotic rate in cardiomyocytes between NC, HG, HG+RES, and HG+RES+UCP2siRNA groups. The apoptotic rate was higher in HG group than that in NC group, and it was lower in HG+RES group than that in HG group ($P < 0.05$, Fig. 7). Notably, apoptotic rate was raised up in HG+RES+UCP2siRNA group compared with that in HG+RES group, which indicated that the protective effect of RES on HG-induced apoptosis is mediated by UCP2.

Discussion

Previous studies suggested that RES could relieve diabetic myocardial fibrosis, but the particular mechanism was incompletely understood. In this study, we revealed that RES treatment protected cardiac function in DCM rats via preventing mitochondrial injury. Moreover, UCP2 mediated the protective effects of RES on mitochondrial function by suppressing the generation of ROS.

In the present study, a rat model of DCM was induced by high-fat diet and STZ intraperitoneal injection. RES showed anti-hyperglycemic and anti-hyperlipidemic effects in diabetic rats in our study. Previous studies have demonstrated that RES improved glucose and lipid metabolism through increasing insulin-dependent glucose transporter 4 (GLUT4) expression [23], enhancing adiponectin level [28], and activating silent information regulatory 2 (Sir2) [36].

Diastolic and systolic dysfunctions were the clinical features of DCM [9, 27], and diastolic dysfunction is one of the first signs of DCM, often developed before systolic dysfunction [10]. Our study showed that RES treatment reversed the impaired diastolic and systolic functions in DCM rats, indicating that there were protective effects of RES not only on advanced cardiac dysfunction, but also on early stage of DCM. Left ventricular hypertrophy and fibrosis are both structure hallmarks of the diabetic hearts. Cardiomyocyte hypertrophy initially develops as an adaptive response to elevated hemodynamic stress [26] and to the lack of normal cardiomyocytes [37]. Myocardial fibrosis, resulting from increased extracellular matrix deposition, impairs myocardial relaxation, subsequently leading to cardiac dysfunction [8]. In the present study, left ventricular hypertrophy and fibrosis were obvious with HE and Masson's trichrome staining in DCM rats, and were significantly suppressed by RES treatment.

Emerging evidences suggested that increased cardiomyocyte apoptosis was important in the pathogenesis of DCM [18]. Cardiomyocyte apoptosis has been observed in the pathogenesis of myocardial fibrosis [11], and is correlated with blood glucose level [17]. Dissipated MMP is a sign of cell early apoptosis, and considered as the "point-of-no-return" in the sequence of events leading to apoptosis [40]. Indeed, in our study, increased cardiomyocyte apoptosis were assessed with TUNEL staining, accompanied with dissipated MMP in DCM rats. And RES treatment inhibited diabetes-induced cardiomyocyte apoptosis and dissipated MMP level. Bcl-2 is thought to be one of the ultimate pathways of apoptosis, as an anti-apoptosis factor [29, 33]. In this study, the up-regulation of Bcl-2 might explain the anti-apoptotic effect of RES in diabetic hearts.

Diabetes-induced mitochondrial dysfunction is a central event in the pathogenesis of DCM. Myocardial energy metabolism disturbances and intracellular ROS accumulation are directly associated with diabetes-induced mitochondrial injury. The disorder of mitochondrial dysfunction activates the pathways leading to cardiomyocyte apoptosis [31]. Thus, prevention of mitochondrial injury from diabetes might be a promising therapeutic target for DCM. RES is considered as a protective agent for mitochondria [7]. RES treatment has been proved protective on myocardial fibrosis and apoptosis in DCM, we hypothesize that the effects of RES are associated with preventing mitochondrial injury from diabetes. In this study, we demonstrated that diabetes-stimulated ROS accumulated in rat heart, and RES attenuated ROS generation in DCM rats.

Antioxidant effects of RES have been pointed in several studies. In an in vitro study, RES inhibited the generation of ROS and regulated the activity of transforming growth factor, thus suppressed proliferation and improved differentiation of myocardial fibroblasts in mice [39]. But the mechanism of antioxidant effect of RES is still unclear. ROS generation is associated with mitochondrial respiratory function. In diabetic hearts, mitochondrial respiratory enzymes, SDH [20], and COX [22] were inactive. In the present study, RES significantly enhanced the activities of SDH and COX, which were suppressed in the DCM rats. These results suggested that the activation of mitochondrial respiratory enzymes by RES contributes to the reduction of ROS generation in DCM rats.

UCP2 is a proton transporter, which is located in the mitochondrial inner membrane. UCP2 can cause H^+ leakage from mitochondrial membrane spaces into the matrix, and reduce the generation of intracellular ROS, thereby regulating mitochondrial function [5, 19]. We assessed the expression of UCP2 by Western blot. It was found that the expression of UCP2 was increased in DCM rats, and was improved further by RES treatment. Consistent with our study, RES was proved to increase the expression of UCP2 in the brain, and protect brain damage caused by stroke [32]. But, whether UCP2 mediated the protective effect of RES is still unknown. And, what's the role of up-regulation of UCP2 in DCM? In this study, we analyzed the effects of UCP2 on mitochondrial function in cardiomyocytes incubated with HG and RES treatment. The effects of RES on inhibiting ROS generation and

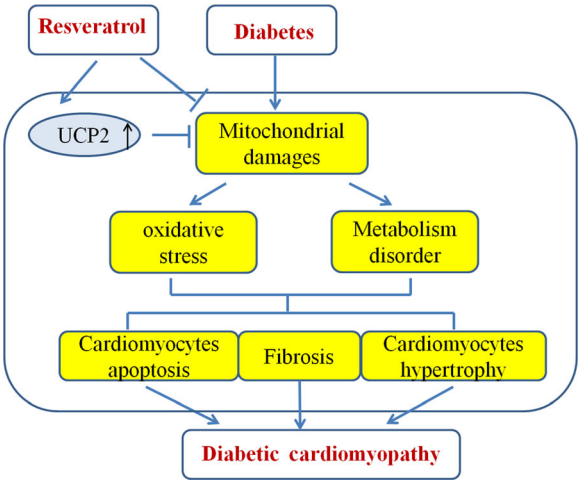

Fig. 8 The possible relationship between DCM, mitochondria damage, UCP2, and RES

the activating respiratory enzymes were both blunted by UCP2siRNA. MPTP is a nonspecific channel in mitochondria, which can be activated by opening ROS, and facilitates Cyto c release from mitochondria [13]. The effects of RES on inhibiting MPTP-sustained opening and Cyto c release were also blunted by suppression of UCP2 expression.

UCP2 has shown anti-apoptotic property in human colon cancer cells under oroxylin condition, which resulted from inhibiting ROS generation [25]. Results from the present study showed that inhibition of UCP2 expression weakened the anti-apoptotic effect of RES in cardiomyocyte incubated with HG. These results suggested that UCP2 mediated the protective effects of RES on mitochondrial function and cardiomyocyte apoptosis. Moreover, the up-regulation of UCP2 in myocardium may be a protective feedback on diabetes-induced mitochondrial injury.

Recently, RES has been used in the clinical treatment of obesity [2], fatty liver [6], and ulcerative colitis [30]. In addition, RES treatment significantly reduced blood lipid levels and suppressed inflammatory response in patients with coronary heart disease [34, 35]. Therefore, as a dietary intervention, RES has potential to become a clinical intervention for diabetes-related cardiovascular diseases, either as a dietary supplement or medicine intervention.

Limits

The animals in the present study were all male. There are many differences between male and female in the pathogenesis of diabetic cardiovascular complications. In this study, we proved that RES ameliorated myocardial mitochondrial and cardiac function in male DCM rats, but whether RES plays the same role in female DCM is not studied. It will be much better to explain the protective effects of RES on DCM if setting-up Control+RES group, but due to time and funding constraints, we did not set-up this group. And we found that UCP2 was up-regulated in myocardium of diabetic rats, but the mechanism of high expression of UCP2 in DCM is still not clear. To confirm these, future research should study the mechanism and effect of up-regulation of UCP2 in DCM, whether it is a protective feedback on mitochondrial injury as we have analyzed.

Conclusion

Taken together, our data demonstrate that RES was able to inhibit myocardial fibrosis and apoptosis, and contributes to the protection of the cardiac function in DCM rats. More importantly, RES ameliorated myocardial mitochondrial function in DCM and UCP2 mediated the effects of RES (Fig. 8). In summary, these results provide overwhelming evidences of the therapeutic potential of RES for DCM, and identify a new insight into the mechanism of RES in protecting mitochondrial function.

Funding information The present study was supported by grant from the Natural Science Foundation of Shannxi (2015JM8431).

Compliance with ethical standards

Conflict of interest The authors declare that there are no conflicts of interest with this work.

References

1. Anderson EJ, Kypson AP, Rodriguez E, Anderson CA, Lehr EJ, Neufer PD (2009) Substrate-specific derangements in mitochondrial metabolism and redox balance in the atrium of the type 2 diabetic human heart. J Am Coll Cardiol 54:1891–1898. https://doi.org/10.1016/j.jacc.2009.07.031
2. Arzola-Paniagua MA, Garcia-Salgado Lopez ER, Calvo-Vargas CG, Guevara-Cruz M (2016) Efficacy of an orlistat-resveratrol combination for weight loss in subjects with obesity: a randomized controlled trial. Obesity (Silver Spring) 24:1454–1463. https://doi.org/10.1002/oby.21523
3. Bonnefont-Rousselot D (2016) Resveratrol and cardiovascular diseases. In: Nutrients. https://doi.org/10.3390/nu8050250
4. Braidy N, Jugder BE, Poljak A, Jayasena T, Mansour H, Nabavi SM, Sachdev P, Grant R (2016) Resveratrol as a potential therapeutic candidate for the treatment and management of Alzheimer's disease. Curr Top Med Chem 16:1951–1960
5. Brand MD, Affourtit C, Esteves TC, Green K, Lambert AJ, Miwa S, Pakay JL, Parker N (2004) Mitochondrial superoxide: production, biological effects, and activation of uncoupling proteins. Free Radic Biol Med 37:755–767. https://doi.org/10.1016/j.freeradbiomed.2004.05.034
6. Chen S, Zhao X, Ran L, Wan J, Wang X, Qin Y, Shu F, Gao Y, Yuan L, Zhang Q, Mi M (2015) Resveratrol improves insulin resistance, glucose and lipid metabolism in patients with non-alcoholic fatty

liver disease: a randomized controlled trial. Dig Liver Dis 47:226–232. https://doi.org/10.1016/j.dld.2014.11.015
7. Csiszar A, Labinskyy N, Pinto JT, Ballabh P, Zhang H, Losonzy G, Pearson K, de Cabo R, Pacher P, Zhang C, Unqvari Z (2009) Resveratrol induces mitochondrial biogenesis in endothelial cells. Am J Physiol Heart Circ Physiol 297:13–20. https://doi.org/10.1152/ajpheart.00368.2009
8. Daniels A, Van Bilsen M, Goldschmeding R, van der Vusse GJ, van Nieuwenhovern FA (2009) Connective tissue growth factor and cardiac fibrosis. Acta Physiol (Oxford) 195:321–338. https://doi.org/10.1111/j.1748-1716.2008.01936.x
9. Devereux RB, Roman MJ, Paranicas M, O'Grady MJ, Lee ET, Welty TK, Fabsitz RR, Robbins D, Rhoades ER, Howard BV (2000) Impact of diabetes on cardiac structure and function: the strong heart study. Circulation 101:2271–2276
10. Do GM, Jung UJ, Park HJ, Kwon EY, Jeon SM, McGregor RA, Choi MS (2012) Resveratrol ameliorates diabetes-related metabolic changes via activation of AMP-activated protein kinase and its downstream targets in db/db mice. Mol Nutr Food Res 56:1282–1291. https://doi.org/10.1002/mnfr.201200067
11. Dong S, Ma W, Hao B, Hu F, Yan L, Yan X, Wang Y, Chen Z, Wang Z (2014) microRNA-21 promotes cardiac fibrosis and development of heart failure with preserved left ventricular ejection fraction by up-regulating Bcl-2. Int J Clin Exp Pathol 7:565–574
12. Duncan JG, Fong JL, Medeiros DM, Finck BN, Kelly DP (2007) Insulin-resistant heart exhibits a mitochondrial biogenic response driven by the peroxisome proliferator-activated receptor-alpha/PGC-1alpha gene regulatory pathway. Circulation 115:909–917. https://doi.org/10.1161/CIRCULATIONAHA.106.662296
13. Elrod JW, Molkentin JD (2013) Physiologic functions of cyclophilin D and the mitochondrial permeability transition pore. Circ J 77:1111–1122
14. Fang ZY, Yuda S, Anderson V, Short L, Case C, Marwick TH (2003) Echocardiographic detection of early diabetic myocardial disease. J Am Coll Cardiol 41:611–617
15. Fang ZY, Prins JB, Marwick TH (2004) Diabetic cardiomyopathy: evidence, mechanisms, and therapeutic implications. Endocr Rev 25:543–567. https://doi.org/10.1210/er.2003-0012
16. Ferraz Da Costa DC, Fialho E, Silva JL (2017) Cancer chemoprevention by resveratrol: the p53 tumor suppressor protein as a promising molecular target. Molecules. https://doi.org/10.3390/molecules22061014
17. Fiordaliso F, Li B, Latini R, Sonnenblick EH, Anversa P, Leri A, Kajstura J (2000) Myocyte death in streptozotocin-induced diabetes in rats in angiotensin II- dependent. Lab Investig 80:513–527
18. Huynh K, Kiriazis H, Du XJ, Love JE, Grav SP, Jandeleit-Dahm KA, McMullen JR, Ritchie RH (2013) Targeting the upregulation of reactive oxygen species subsequent to hyperglycemia prevents type 1 diabetic cardiomyopathy in mice. Free Radic Biol Med 60:307–317. https://doi.org/10.1016/j.freeradbiomed.2013.02.021
19. Krauss S, Zhang CY, Lowell BB (2005) The mitochondrial uncoupling-protein homologues. Nat Rev Mol Cell Biol 6:248–261. https://doi.org/10.1038/nrm1572
20. Lashin OM, Szweda PA, Szweda LI, Romani AM (2006) Decreased complex II respiration and HNE-modified SDH subunit in diabetic heart. Free Radic Biol Med 40:886–896. https://doi.org/10.1016/j.freeradbiomed.2005.10.040
21. Ma J, Banerjee P, Whelan SA, Liu T, Wei AC, Ramirez-Correa G, McComb ME, Costello CE, O'Rourke B, Murphy A, Hart GW (2016) Comparative proteomics reveals dysregulated mitochondrial O-GlcNAcylation in diabetic hearts. J Proteome Res 15:2254–2264. https://doi.org/10.1021/acs.jproteome.6b00250
22. Nakamura H, Matoba S, Iwai-Kanai E, Kimata M, Hoshino A, Nakaoka M, Katamura M, Okawa Y, Ariyoshi M, Mita Y, Ikeda K, Okigaki M, Adachi S, Tanaka H, Takamatsu T, Matsubara H (2012) p53 promotes cardiac dysfunction in diabetic mellitus caused by excessive mitochondrial respiration-mediated reactive oxygen species generation and lipid accumulation. Circ Heart Fail 5:106–115. https://doi.org/10.1161/CIRCHEARTFAILURE.111.961565
23. Palsamy P, Subramanian S (2010) Ameliorative potential of resveratrol on proinflammatory cytokines, hyperglycemia mediated oxidative stress, and pancreatic beta-cell dysfunction in streptozotocin-nicotinamide-induced diabetic rats. J Cell Physiol 224:423–432
24. Pohjoism äki JL, Goffart S (2017) The role of mitochondria in cardiac development and protection. Free Radic Biol Med 106:345–354. https://doi.org/10.1016/j.freeradbiomed.2017.02.032
25. Qiao C, Wei L, Dai Q, Zhou Y, Yin Q, Li Z, Xiao Y, Guo Q, Lu N (2015) UCP2-related mitochondrial pathway participates in oroxylin A-induced apoptosis in human colon cancer cells. J Cell Physiol 230:1054–1063. https://doi.org/10.1002/jcp.24833
26. Ritchie RH, Irvine JC, Rosenkranz AC, Patel R, Wendt IR, Horowitz JD, Kemp-Harper BK (2009) Exploiting cGMP-based therapies for the prevention of left ventricular hypertrophy: NO* and beyond. Pharmacol Ther 124:279–300. https://doi.org/10.1016/j.pharmthera.2009.08.001
27. Rubler S, Dlugash J, Yuceoglu YZ, Kumral T, Branwood AW, Grishman A (1972) New type of cardiomyopathy associated with diabetic glomerulosclerosis. Am J Cardiol 30:595–602
28. Rui Y, Cheng J, Qin L, Shan C, Chang J, Wang G, Wan Z (2017) Effects of vitamin D and resveratrol on metabolic associated markers in liver and adipose tissue from SAMP8 mice. Exp Gerontol 93:16–28. https://doi.org/10.1016/j.exger.2017.03.017
29. Safaeian L, Abed A, Vaseghi G (2014) The role of Bcl-2 family proteins in pulmonary fibrosis. Eur J Pharmacol 741:281–289. https://doi.org/10.1016/j.ejphar.2014.07.029
30. Samsami-Kor M, Daryani NE, Asl PR, Hekmatdoost A (2015) Anti-inflammatory effects of resveratrol in patients with ulcerative colitis: a randomized, double-blind, placebo-controlled pilot study. Arch Med Res 46:280–285. https://doi.org/10.1016/j.arcmed.2015.05.005
31. Schilling JD (2015) The mitochondria in diabetic heart failure: from pathogenesis to therapeutic promise. Antioxid Redox Signal 22:1515–1526. https://doi.org/10.1089/ars.2015.6294
32. Shin JA, Lee KE, Kim HS, Park EM (2012) Acute resveratrol treatment modulates multiple signaling pathways in the ischemic brain. Neurochem Res 37:2686–2696. https://doi.org/10.1007/s11064-012-0858-2
33. Shiomi T, Tsutsui H, Ikeuchi M, Matsusaka H, Hayashidani S, Suematsu N, Kubota T, Takeshita A (2003) Streptocin-induced hyperglycemia exacerbates left ventricular remodeling and failure after experimental myocardial infarction. J Am Coll Cardiol 42:165–172
34. Tome-Carneiro J, Gonzalvez M, Larrosa M, Yáñez-Gascón MJ, García-Almagro FJ, Ruiz-Ros JA, García-Conesa MT, Tomás-Barberán FA, Espín JC (2012) One-year consumption of a grape nutraceutical containing resveratrol improves the inflammatory and fibrinolytic status of patients in primary prevention of cardiovascular disease. Am J Cardiol 110:356–363. https://doi.org/10.1016/j.amjcard.2012.03.030
35. Tome-Carneiro J, Gonzalvez M, Larrosa M, Yáñez-Gascón MJ, García-Almagro FJ, Ruiz-Ros JA, Tomás-Barberán FA, García-Conesa MT, Espín JC (2013) Grape resveratrol increases serum adiponectin and downregulates inflammatory genes in peripheral blood mononuclear cells: a triple-blind, placebo-controlled, one-year clinical trial in patients with stable coronary artery disease. Cardiovasc Drugs Ther 27:37–48. https://doi.org/10.1007/s10557-012-6427-8
36. Valenzano DR, Terzibasi E, Genade T, Cattaneo A, Domenici L, Cellerino A (2006) Resveratrol prolongs lifespan and retards the

onset of age-related markers in a short-lived vertebrate. Curr Biol 16:296–300. https://doi.org/10.1016/j.cub.2005.12.038

37. Van Empel VP, De Windt LJ (2004) Myocyte hypertrophy and apoptosis: a balancing act. Cardiovasc Res 63:487–499. https://doi.org/10.1016/j.cardiores.2004.02.013
38. Victor VM, Rocha M, Herance R, Hernandez-Mijares A (2011) Oxidative stress and mitochondrial dysfunction in type 2 diabetes. Curr Pharm Des 17:3947–3958
39. Wu H, Li GN, Xie J, Li R, Chen QH, Chen JZ, Wei ZH, Kang LN, Xu B (2016) Resveratrol ameliorates myocardial fibrosis by inhibiting ROS/ERK/TGF-beta/periostin pathway in STZ-induced diabetic mice. BMC Cardiovasc Disord. https://doi.org/10.1186/s12872-015-0169-z.16: 5
40. Zamzami N, Kroemer G (2003) Apoptosis: mitochondrial membrane permeabilization–the (w)hole story? Curr Biol 13:71–73